Ultrafast Microfluidic Droplet Sorter Extension Work

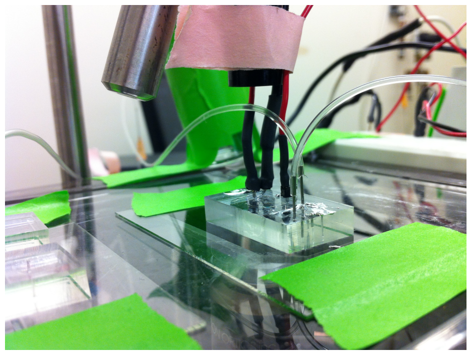

Luke Kong

Samuel Wu

Project Sponsor:

Dr. Carl Hansen

Project Mentors:

Tim Leaver

Adam Quiring

ENPH 459

Engineering Physics

The University of British Columbia

April 2, 2012

Project Number 1209

Executive Summary

This project builds on work done by a previous APSC 459 group, who developed fluorescence-based droplet sorting device similar to that described by Agresti et al. up to the point where it could detect the fluorescence of droplets up to a rate of 1kHz. However, it was unable to sort droplets; this project sought to add droplet sorting functionality to their microfluidic chip design.

Our project aimed to demonstrate droplet actuation with use of the existing experimental setup. This consisted of three main objectives:

1. Model effect of electrode design and geometry on droplet actuation using finite-element analysis (implemented in COMSOL).
2. Demonstrate actuation of droplets, redesigning microfluidic chip if necessary.
3. Optimize setup towards droplet sorting at speeds on the same order (1-2 kHz) as existing work (Agresti, 2010).

Using COMSOL we determined the factors that will most strongly affect the dielectrophoretic force on a droplet in a channel. From these results we redesigned the droplet sorter chip from the previous group and fabricated chips with a new electrode design (microfluidic channels to be filled with low-melting-point alloy). We then went on to demonstrate droplet redirection at a rate of at least 100Hz.

Although droplet redirection, the main focus of this project, was successfully demonstrated, much work remains to be done on this project. The redirection needs to be coupled to the previous 459 group's droplet detection setup in order for controlled droplet actuation. Recommendations were made about electrode fabrication, droplet transfer from generator to sorter and high voltage switching.

Table of Contents

Table of Figures / Tables

1.0 Introduction

Our ever-growing understanding of biology allows us to manipulate and engineer biological systems in novel ways, with such fields as synthetic biology and protein engineering. As biology operates on small scales (proteins to cells) and across large orders of magnitudes (trillions of molecules/cells), effective assaying techniques are essential for successful experimentation and validation. Screening, however, is often a rate-limiting step in both time and resources.

Existing macro-assaying methods involving microwell plates, when automated robotically, can achieve processing speeds of ~1 Hz, but this does not allow for treatment of individual cells (Agresti et al., 2010).

Optimally, it is desired to be able to manipulating individual cells in a high throughput manner, requiring technology capable of operating on small size scales. Encapsulation of biomaterial within droplets provides such a platform, allowing for treatment within a unique picolitre scale microenvironment. Each droplet could potentially be experimented upon individually, able to be split and merged with other droplets (Griffiths & Tawfik, 2006).

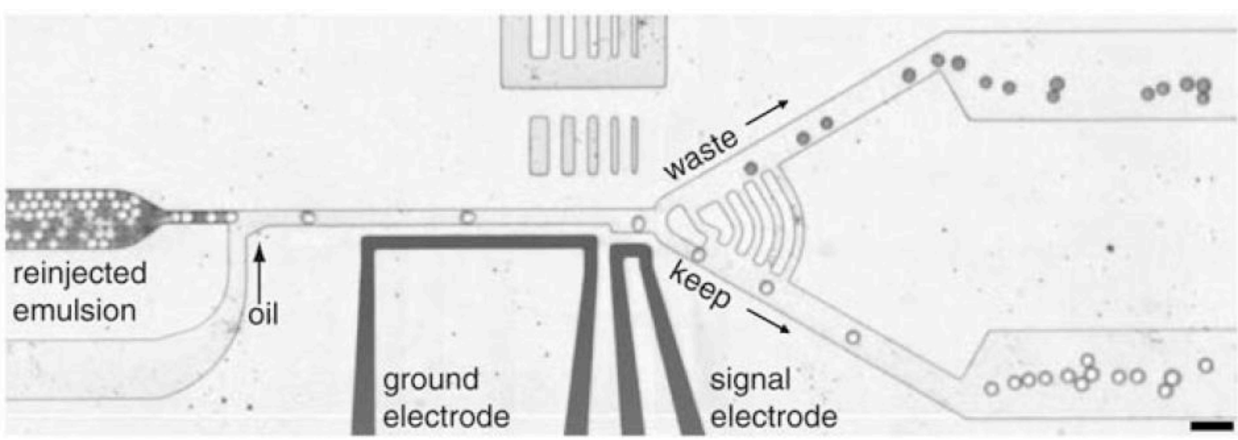

Fig. 1Diagram of microfluidic droplet sorter. Fluorescent droplets are seen here as light-colored spheres, non-fluorescent drops as dark. (Agresti et al., 2010)

Sponsored by Dr. Carl Hansen (UBC Centre for High-Throughput Biology), this project aims to replicate a droplet sorter developed by Agresti et al. They were able to sort droplets into one of two channels by applying a voltage across two electrodes, creating a non-uniform electric field and a subsequent dielectrophoretic force on the droplet.

If successful, this device could be applied towards directed evolution or digital PCR experiments, potentially reducing time and reagent costs by several orders of magnitude.

The project objective, as stated by the project sponsor Carl Hansen:

> **"**Add droplet sorting functionality to the microfluidic chip. This should be accomplished by adding an electrode upstream of a junction leading to two collection channels. By using the electrode to apply an electric field across the channel, droplets could be sorted into one of the two channels. The group would be required to research and design the electrodes (as well as selecting a suitable fabrication technique) as well as the switching electronics. This objective could involve modeling in COMSOL and microfabrication of test devices."

In addition, we had three self-formed project objectives:

1. Model electrode design with COMSOL

   We will model the effect of electrode design on actuation of droplets using COMSOL (finite-element analysis). Varying different factors (electrode position, geometry, AC vs. DC field, field strength), we will produce an evaluation for the electrode design which will exert the maximum dielectrophoretic force on a 25 µm-diameter droplet.

2. Demonstrate droplet actuation.

   We will demonstrate actuation of droplets using the electrode design chosen from the modelling, redesigning the microfluidic chip if necessary. Sorting will be performed at 1Hz at this stage, as demonstrating that actuation is controllable and reproducible is the main focus of this objective.

3. Optimize droplet sorting.

Improve experimental setup towards sorting at speeds on the same order (1-2 kHz) as existing work (Agresti, 2010).

This report will outline the theory used, the methods and results of various experiments, issues encountered, as well as conclusions and recommendations for future developments regarding this project. This report aims to convey project findings to the project sponsor, Carl Hansen, his lab personnel and the Engineering Physics Project Lab.

2.0 Discussion

2.1 Dielectrophoresis

Particles present in an applied electric field exhibit polarization; when placed in a non-uniform electric field, the particle will be subject to a dielectrophoretic force. Depending on a difference in electric properties (i.e. dielectric constant), a water droplet present in an oil will move towards an area of higher electric field, experiencing a force given by the following relation (Ahn et al., 2006):

$$F_{DEP} = 4\pi r^3 \nabla \left| \vec{E} \right|^2$$

Dielectrophoresis is the actuation mechanism for sorting droplets. However, if a DC voltage is applied screening effects, where the environment around a polarized particle polarizes in the opposite direction to offset the charge accumulation, reduce the effective electric field. This can be negated by applying an AC signal on the order of 20kHz (Agresti et al., 2010). Thus, a high voltage 20kHz AC signal of at least 1kV across the electrodes is desired.

2.2 High-Voltage Switching

To produce a HV AC signal, a suitable switching mechanism was required to handle voltages of at least 1kV. The voltage itself is provided by a PS325 2500V-25W high voltage power supply made by Stanford Research Systems, Inc.

A solid state switch from Behlke meeting technical requirements (HTS 61-03-GSM - rise/fall time of 10ns, maximum operating frequency of 2.5MHz) was identified and subsequently ordered, but due to a number of complications on part of the company we were not able to obtain the switch (Behlke, 2012). A switch designed and constructed by the PHAS E-LAB was fortunately able to be obtained from Pavel Trochtchanovitch (E-LAB manager). This switch is driven by a 0-5V signal and can handle switching voltages of up to 3kV. A schematic of the switch can be found in Appendix C.

The electrodes were characterized in order to determine if they possessed any parasitic capacitance which would limit the maximum frequency of the applied AC signal. The switch was characterized to determine performance with our system.

2.3 Modeling

The cell sorter system is modeled on COMSOL Multiphysics software prior to its fabrication. The governing formula for the dielectrophoretic force: $F_{DEP} = 4\pi r^3 \nabla \left|\vec{E}\right|^2$ is a function of the gradient of the electric field squared. The goal is to optimize the system on the software to maximize $\nabla \left|\vec{E}\right|^2$.

2.3.1 The Construct

This system contains three important components: Component 1 being the oil channel, where the droplets travel; Component 2 represents the ground electrode; Component 3 is the high voltage electrode. These three components are in the same x-y plane. Above this plane, lies the PDMS top, and the glass base is settled below it.

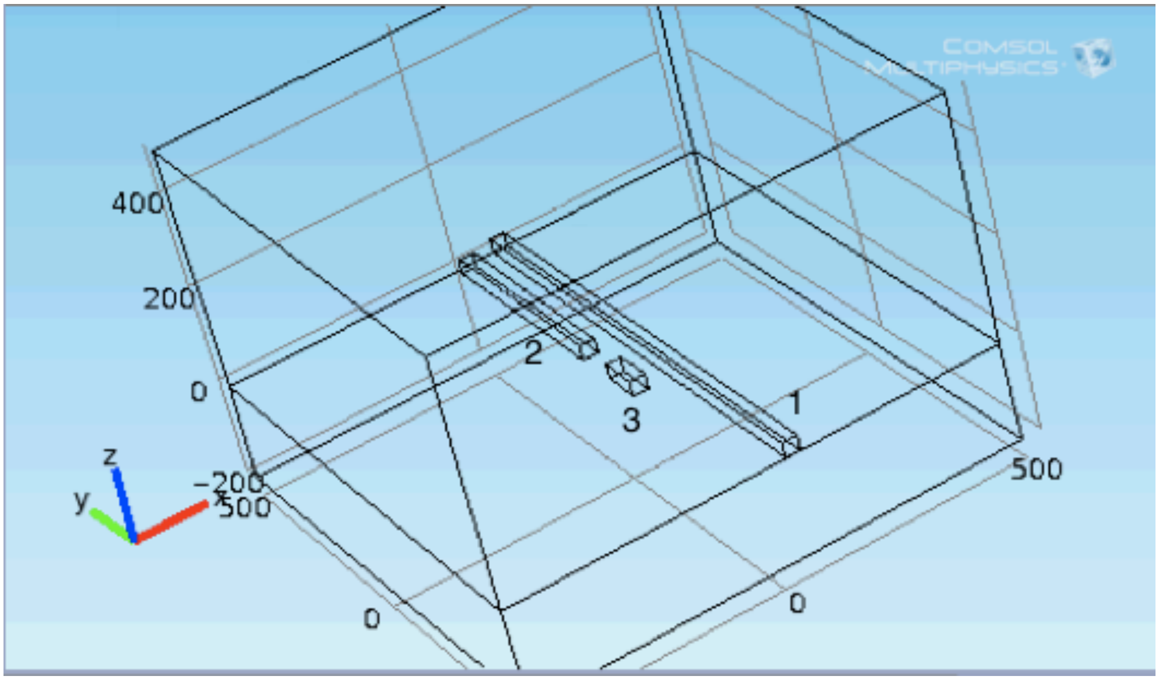

Fig. 2. Basic construct of COMSOL electrode model

There are a few parameters to be tested in this stage. By speculation, the most influential parameter would be the distance between the electrodes and the oil channel in the x-direction (d_1). Secondary concerns are the distance between the electrodes in the y-direction (d_2), and the thickness of the electrodes (d_3).

2.3.2 Finite Element Analysis

The modeling process provides a wide range of accuracies. COMSOL basically breaks this system into tens or hundreds of thousands of tetrahedrons and analyze each element individually. To achieve an accurate estimate, it is necessary to have a higher density near the electrodes and the oil channel, whereas the states of the regions far away do not contribute much to the accuracy of the calculation. The system is therefore broken down in this manner:

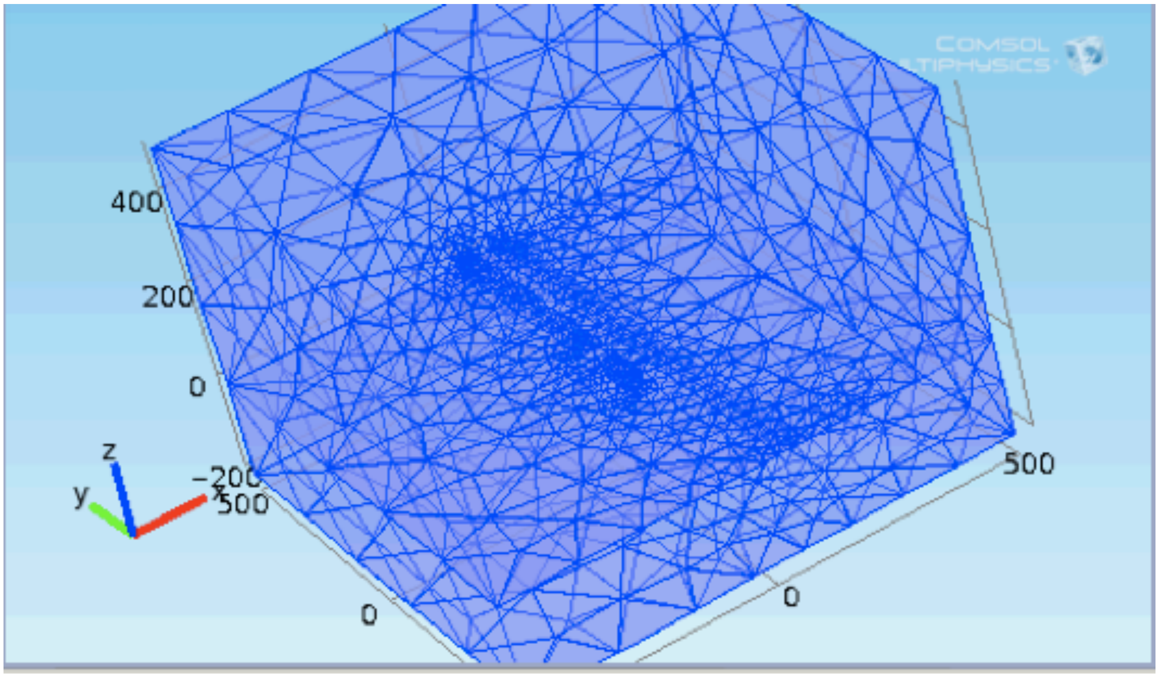

Fig. 3. Mesh for COMSOL electrode model

2.3.4 Computation

Although the entire system is analyzed, it is only the region near the oil channel is of interest. Therefore, a y-z study plane cutting through the oil channel is created to display the information in a more clarified style:

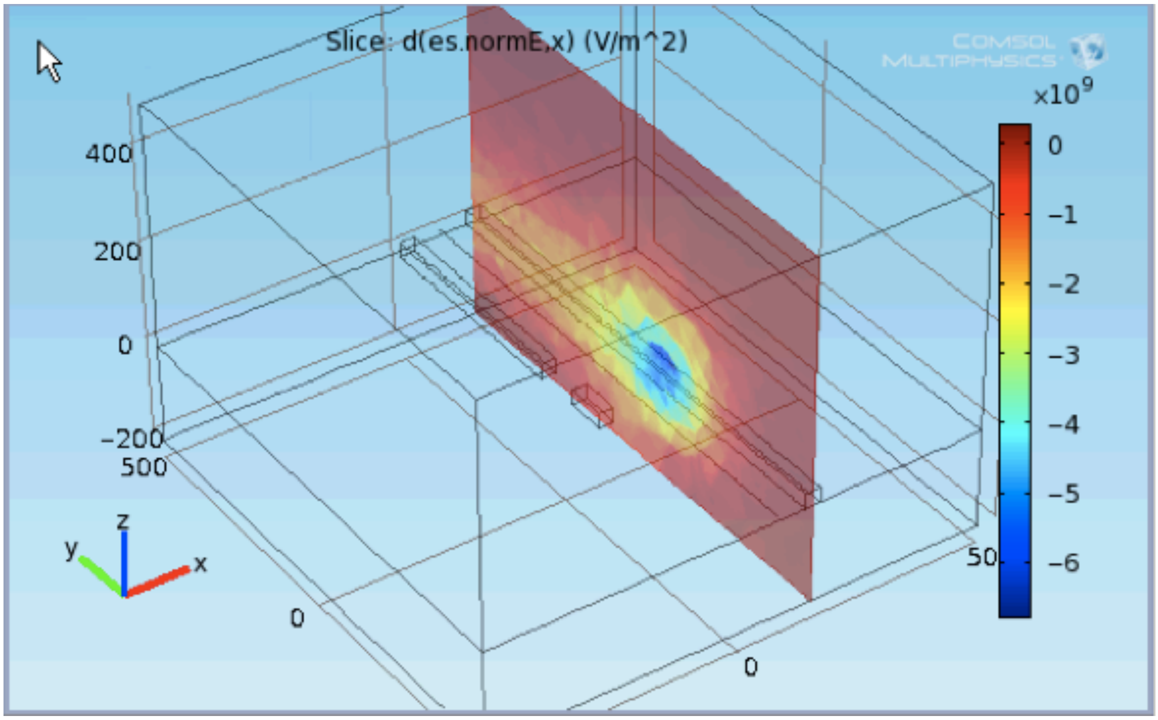

Fig. 4. Y-Z slice study of $\nabla|\vec{E}|^2$ halfway through oil channel in x direction.

In the figure above, the colours represent the strength of the divergence of E-norm squared in the x-direction. The colour darkens as the strength increases, as indicated by the scale bar. The maximum value occurs in the area of the oil channel perpendicular to the signal electrode.

2.3.5 Optimization

The task now is to vary electrode spacing and optimize this parameter. The procedure involves manually decrement the value of a parameter that determines d_1, starting from the original distance used in the previous group's design. After plotting the results on Excel, it is concluded that the gradient increases as d_1 decreases.

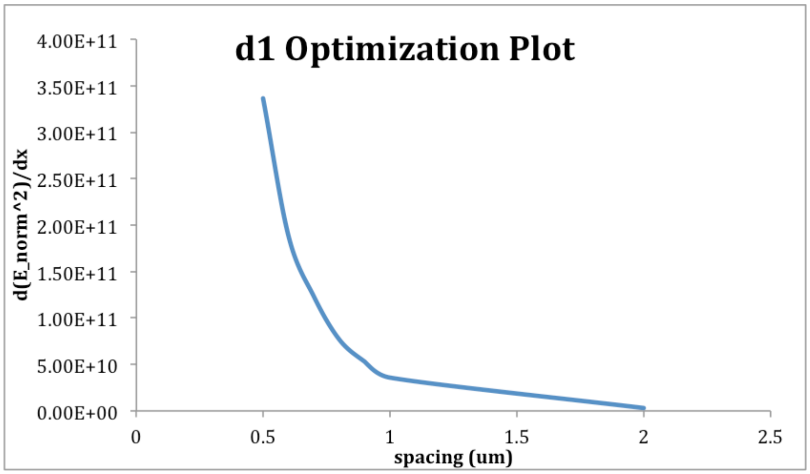

Fig. 5. Plot of $\nabla\left|\vec{E}\right|^2$ as a function of electrode spacing d_1

According to the data, the gradient strength increased 100 times, as d_1 is decreased to a fourth of its original value. The eventual best result obtained is $d_1 = 7\mu m$ giving $\nabla\left|\vec{E}\right|^2 = 3.77\times10^{11}$.

The absolute potential difference is at 500 V, in DC setting. The secondary parameters are then tested, and they demonstrated little contribution to the gradient strength. Due to fabrication limitations, these parameters are given rather modest values, which will be elaborated upon in the next section of this report.

2.4 Sorter Chip Design

The chip design is inherited from the AutoCAD file drawn by the previous group. The design demonstrated a close resemblance to the original design by Agresti et al. However, critical changes are applied according to the COMSOL model to maintain consistency. The AutoCAD file can be found on the USB stick included with this report.

2.4.1 List of Modifications

1. Channels for the electrodes are added
2. Inlets and outlets are added to allow the liquid form of the metal alloy to flow into the channels and solidify
3. Replaced the second design with the current design to have in total 8 similar chips on a single wafer

2.4.2 Design Description

One silicone wafer is able to hold designs for eight PDMS chips. Four different designs are used, resulting in two chips per design. Therefore, some less optimal designs are included in the intention of result comparison. The core design, inherited from the COMSOL model plus three other variations make up the four designs. Due to fabrication limitations, the parameter d_1 as described in Section 3, has been increased to $10\mu m$.

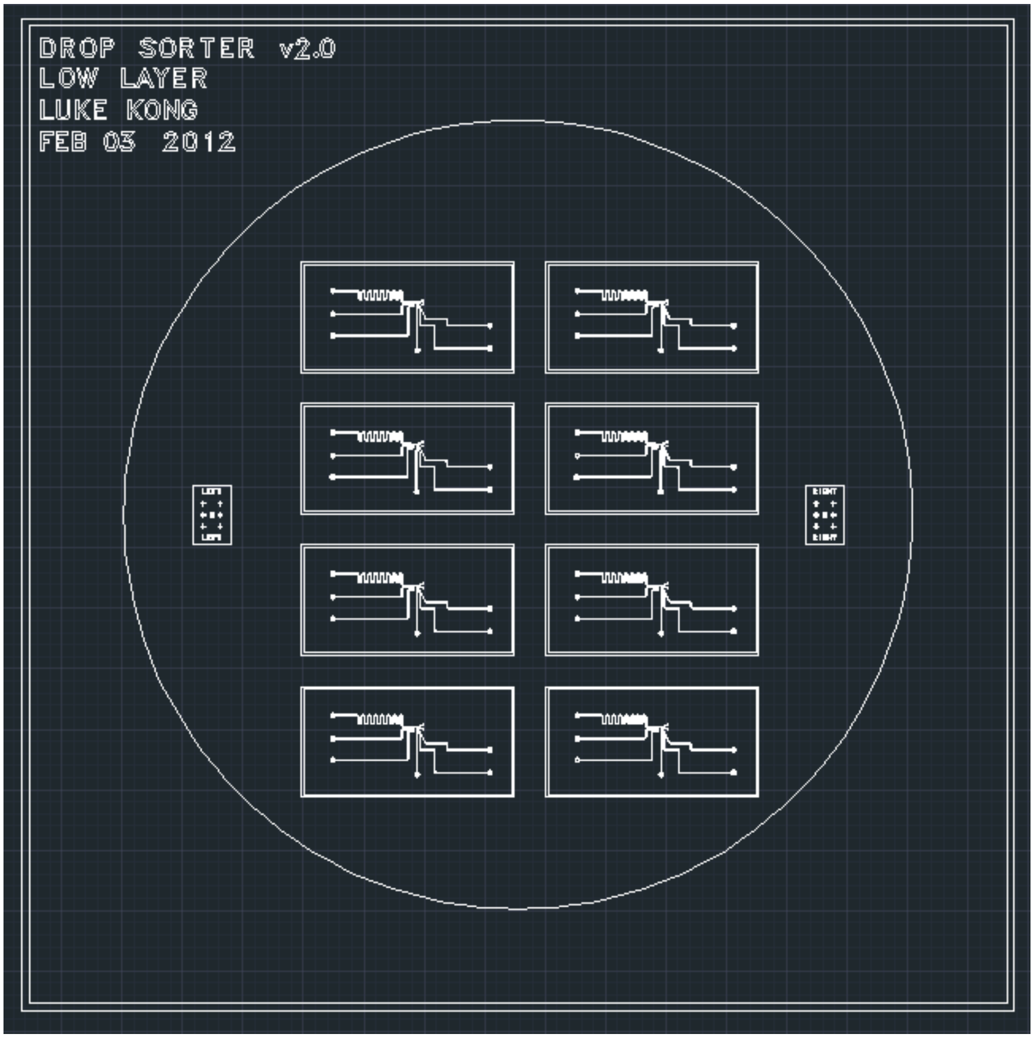

Fig. 5. AutoCAD drawing of droplet sorter chips.

Table 1: Droplet Sorter Design Specifications

Design	d_1 (μm)	d_2 (μm)
1	10	72
2	10	142
3	20	72
4	10	110

As stated in the Table 3.01, d_1 in the third design is twice the magnitude of the others. It is to confirm the results predicted by computer modeling discussed in Section 4. The fourth design is rather unconventional. It is suspected that the electrode with a sharp end may produce a more powerful electric field. This idea is then implemented in the AutoCAD design for testing purposes.

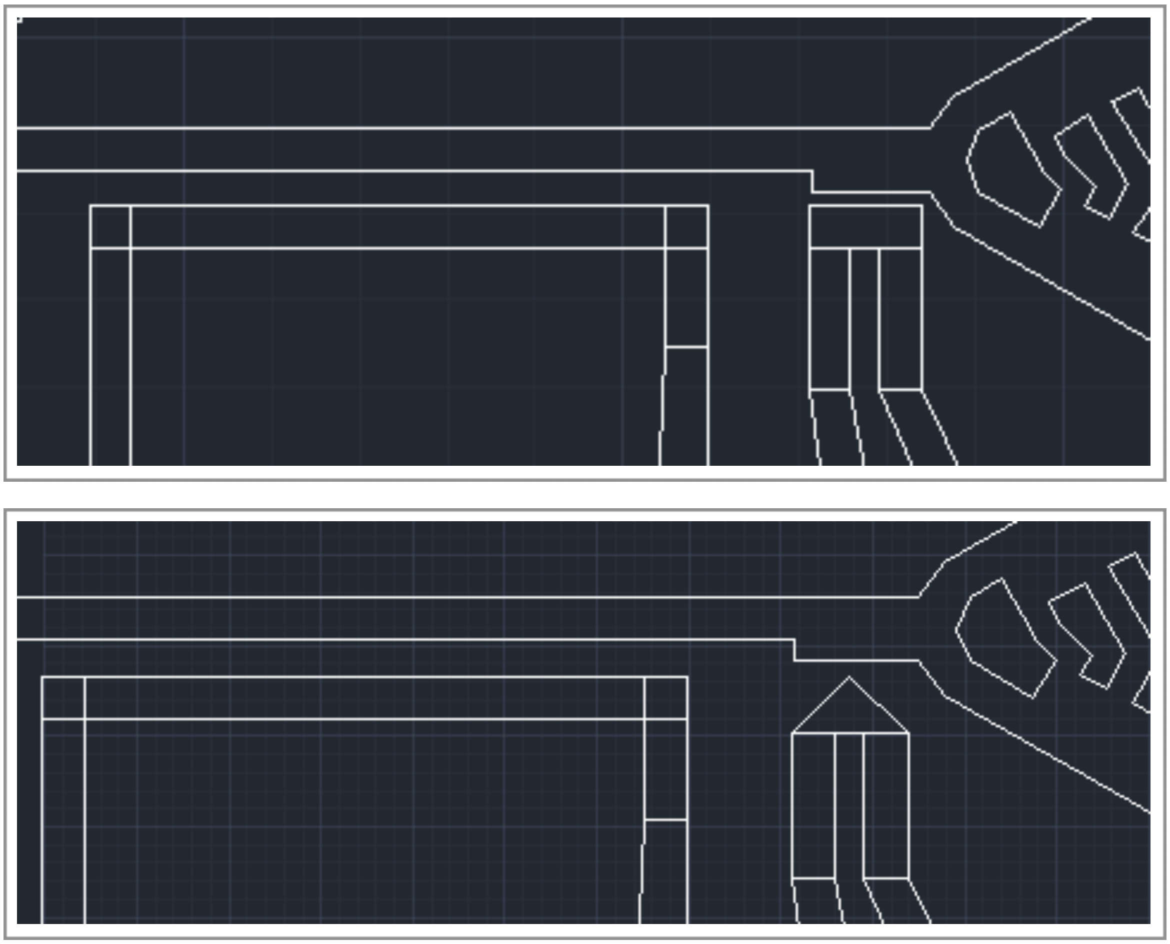

Fig. 6. Flat (top) and sharp (bottom) electrode designs.

2.5 Sorter Chip Fabrication

2.5.1 Fabrication

Fabrication was performed with the microfabrication facilities in the NCE cleanroom, UBC. The process took in total 4 days. Detailed protocols can be found in Appendix A.

2.5.2 Results

Two wafers were fabricated and the specifications listed in Table 4.01. Variations in channel height occurred due to slight differences in UV exposure time and fabrication errors (missing UV filter, etc.).

Table 2: Photoresist specifications

Wafer 1	Height (µm)	Width (µm)
Output Channel	130	180
Oil Channel	40	30
Electrode	40	30

Wafer 2	Height (µm)	Width (µm)
Output Channel	142	185
Oil Channel	50	30
Electrode	50	30

2.6 Electrode Fabrication

The previous group fabricated electrodes with etched chrome placed below the PDMS sorter chip, contrary to what was done in the Agresti paper, where channels were formed alongside that of the sorter and filled with a low-melting point solder. We opted to follow the method in the Agresti paper, adding channels to the previous sorter chip design.

Several low-melting-point alloys were considered, but due to price, eutectic Gallium Indium was chosen. As it is liquid at room temperature, it can be injected into the channel inlets with a syringe. Quotes from Indium and AIM Solder can be found in Appendix D.

2.6.1 Procedure

The liquid GaIn is withdrawn into a 1mL syringe and injected into the one of the electrode channel inlets.

2.6.2 Results

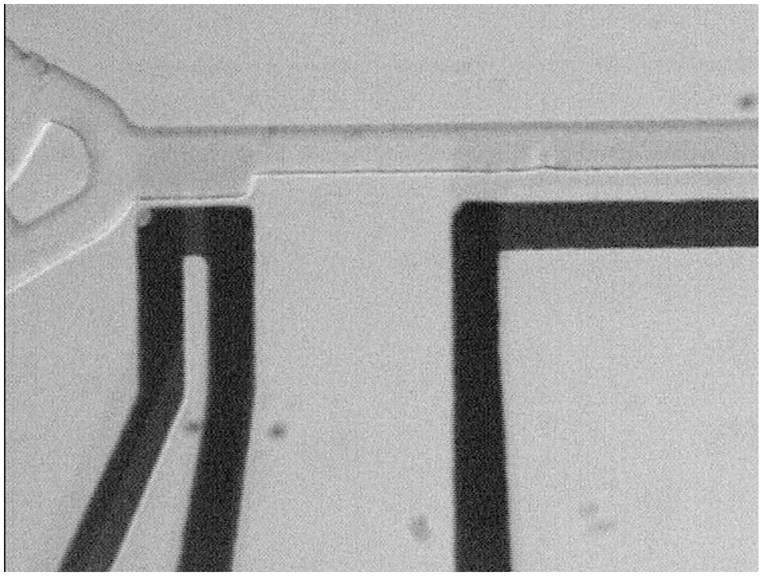

Fig. 7 Electrode channels following injection of GaIn

GaIn seemed to flow well through the PDMS channels, requiring only minimal back pressure applied to the syringe. It adheres well to the channel walls and fills the channel completely with no problems at corners or air bubbles without any need of priming.

However, due to high surface tension forces, upon removal of syringe from electrode channel inlet a large amount of GaIn will spill out. As it does not spread out over a surface at room temperature, the majority can be withdrawn back into the syringe and the residue can be cleaned off by water or HFE-7500 oil, but it cannot be removed completely.

2.7 Electrode Characterization

Electrodes were tested to determine their ability to conduct an AC signal by determining the RC time constant. This time constant was assumed to be independent of the voltage applied (resistance and capacitance being properties of the material).

2.7.1 Procedure

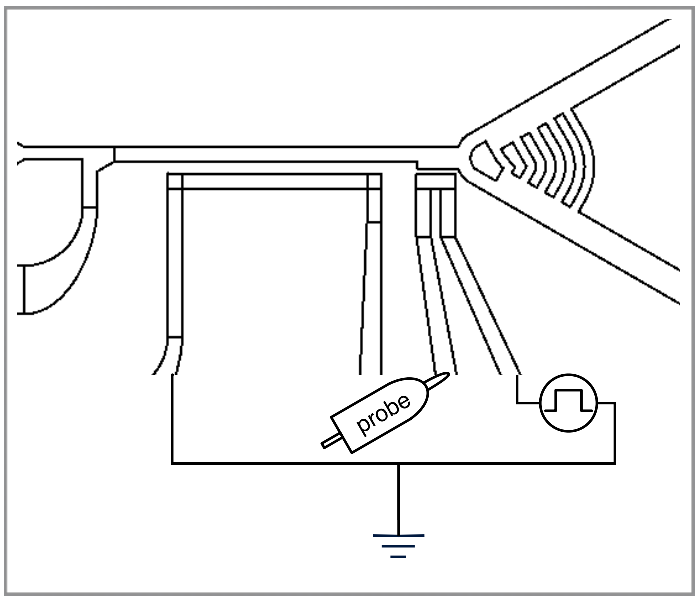

Fig. 8. Diagram of setup for electrode characterization.

1. A 0-6V square wave was applied with the NI DAQ card to the signal electrode inlet and the output signal measured at the signal electrode outlet.
2. Square waves at 200Hz, 20kHz and 1MHz were applied to the electrode inlet and the time constant was measured using the OSCILLOSCOPE to be the time taken for the voltage at the electrode outlet to reach $\frac{1}{e}$ of its original value at the falling edge.

2.7.2 Results

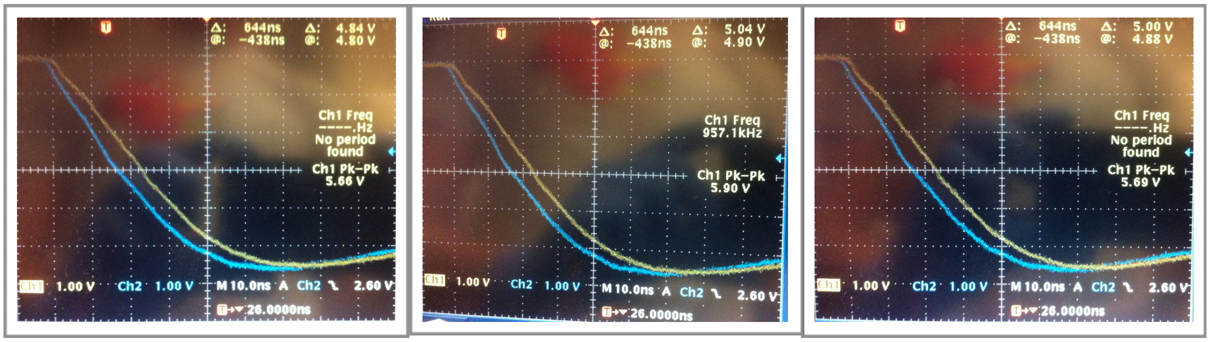

Fig 9. Electrode voltage (yellow) when a 0-5V square wave (200Hz, 20kHz, 1MHz left to right) is applied (blue)

The time constant at the signal electrode was measured to be 30ns at each applied frequency, while that of the applied TTL signal was 25ns. The electrode signal closely follows the applied voltage waveform, suggesting that maximum switching frequency across the electrodes is limited by the applied signal, not necessarily by the electrode's capacitance.

This suggests a maximum frequency of at least 33MHz, well above that of the desired 20kHz. The maximum should theoretically be even higher, since the electrode time constant seemed to be dependent on the signal time constant.

2.8 Switch Characterization

The switch was characterized to determine performance with our system.

2.8.1 Procedure

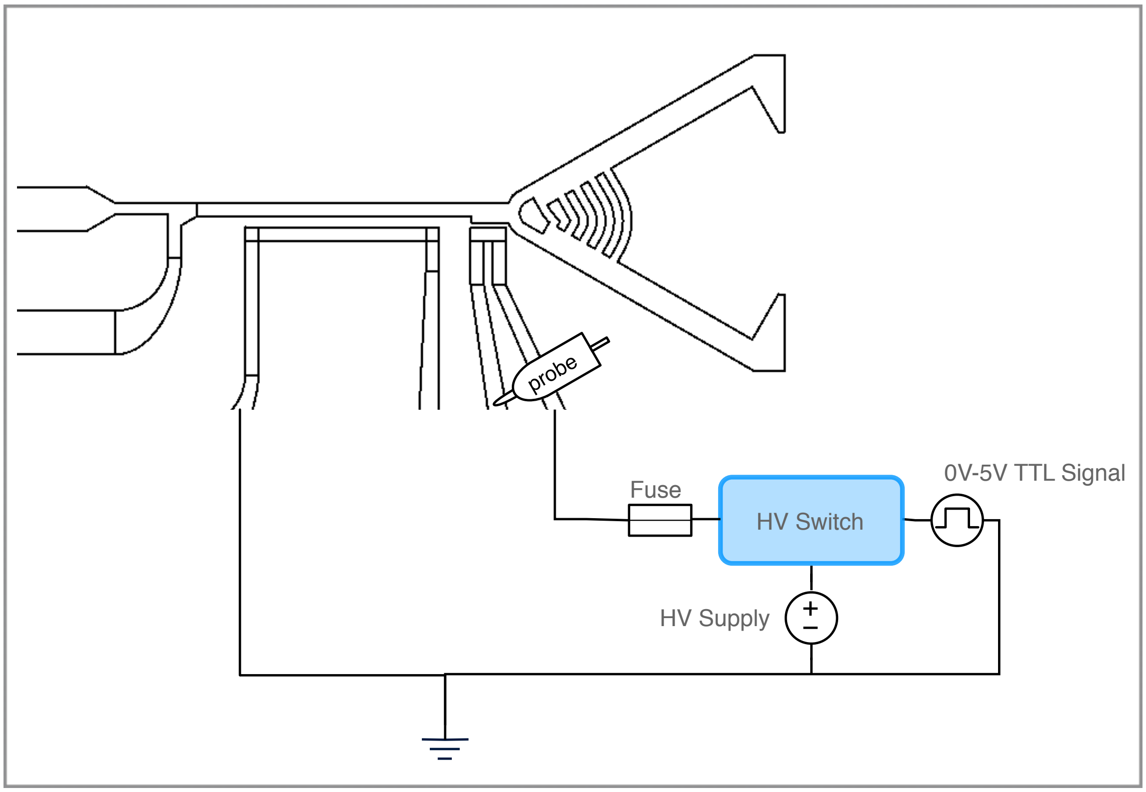

Fig. 10. Schematic for connecting HV supply to electrodes

1. A 10V signal (from HV source) was applied to the electrodes at 400Hz, 1kHz, 20kHz and the switch output measured on the scope.
2. A 75V AC signal was applied to the electrodes at 800Hz, 1kHz and 20kHz and the switch output measured.
3. 50V, 100V, 200V and 300V were applied to the switch and the output measured with a high-voltage probe (which reduces a voltage by 1220x to be readable on the scope). Due to some yet unknown reason, the high-voltage probe was only able to make measurements when a regular scope probe was also attached to the switch output, therefore only voltages up to 300V (maximum rating for the regular probe) were able to be tested.

2.8.2 Results

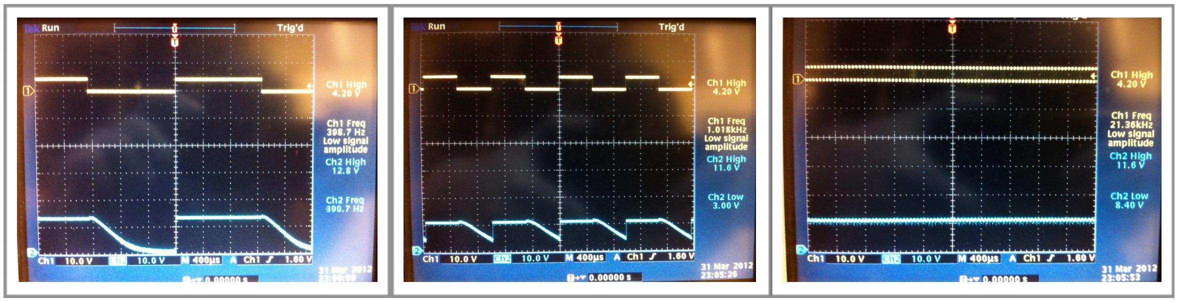

Fig. 11. Switch output (blue) with 10V signal applied at input (yellow) at 400Hz, 1kHz and 20kHz left to right

Output signal exhibits a long fall time, which results in the signal being clipped starting at around 500Hz. At 20kHz the voltage is similar to that of a DC voltage signal.

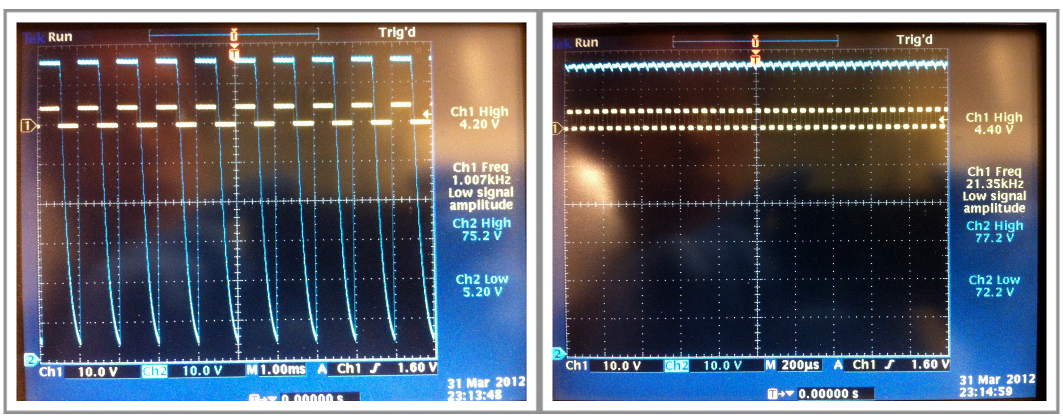

Fig. 12. Switch output (blue) with 75V signal applied at input (yellow) at 1kHz and 20kHz left to right

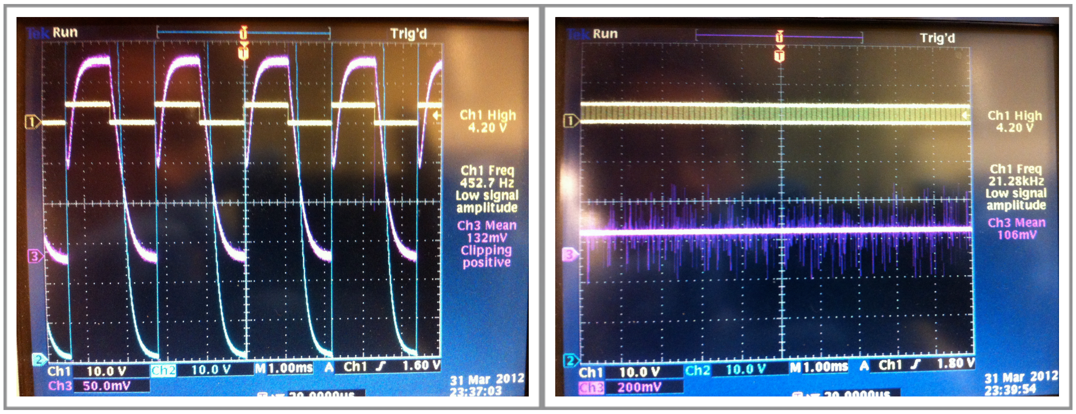

Fig. 13. Switch output measured by high-voltage probe (purple) and regular oscilloscope probe (blue) when 300V signal is applied at 450Hz and 20kHz

The output when 75V and 300V is applied exhibits a similar behavior to that of 10V, with the falling edge clipping upwards until it is similar to a DC signal at 20kHz. The switch can therefore be operated in AC up to 1kHz before clipping becomes a large factor and operating the switch at 20kHz can let us mimic a DC signal.

2.9 Droplet Actuation

Droplets were formed using the existing implementation (Fig. 2); a PDMS device connected to input syringe pumps coflows HFE-7500 oil with 3% w/w PFPE-PEG block copolymer surfactant (to prevent droplet coalescence) to disperse the aqueous droplets at the flow-focusing junction (inset). These droplets were then collected in a microcentrifuge tube from the output port and re-injected into the sorting device (Mulholland et al., 2011).

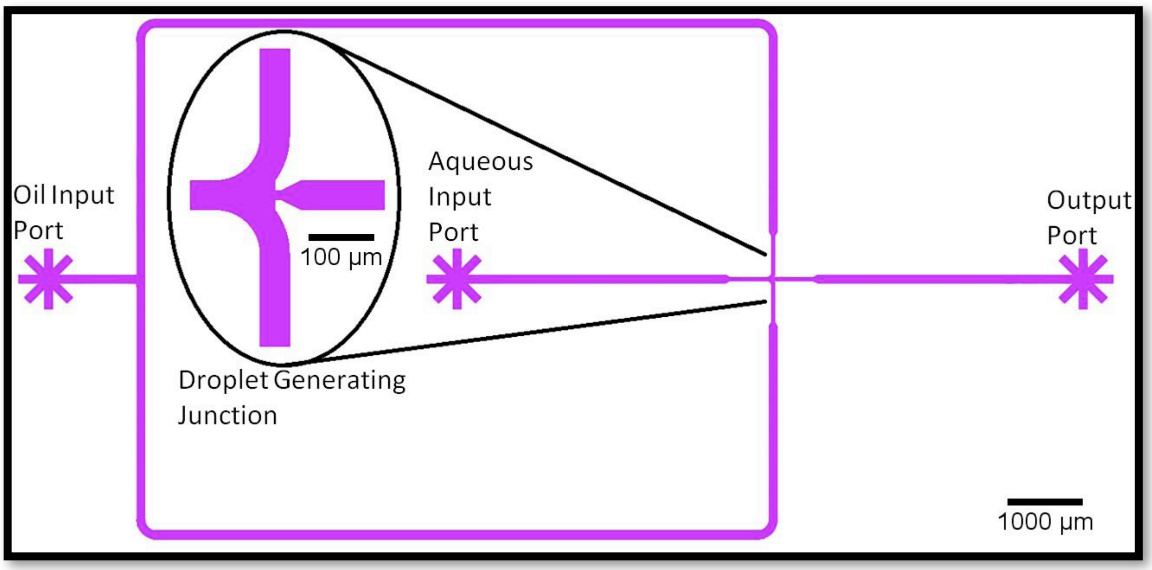

Fig. 14. Droplet generating device generated by previous APSC 459 group (Mulholland et al., 2011).

The sharp and flat electrode designs were tested at a range of voltages and applied frequencies, with actuation detected t 30 fps by the CCD camera setup developed by the previous 459 group. The high-voltage source is connected to the switch via a high-voltage connector and the switch is driven by a 0-5V TTL signal from the NI DAQ board. The switch output is connected to the signal electrode through a 200mA fuse and the ground electrode is connected to ground.

2.9.1 Procedure

1. 30um droplets were formed using 20-67-31 (D1-D2-Height) droplet generator chip flowing HFE-7500 with 3% w/w RainDance surfactant at 250uL/hr and deionized water at 25uL/hr.
2. Droplets were withdrawn into a 1mL syringe and re-injected into the sorter chip with sharp electrode design at 10uL/hr with an accompanying oil flow rate of 100uL/hr.
3. A HV AC signal was applied to electrodes via switch at 500V, 1000V, 2000V, 2500V with frequencies 500Hz, 1kHz, 20kHz.

An SOP for generating droplets used with this test can be found in Appendix B.

2.9.2 Results

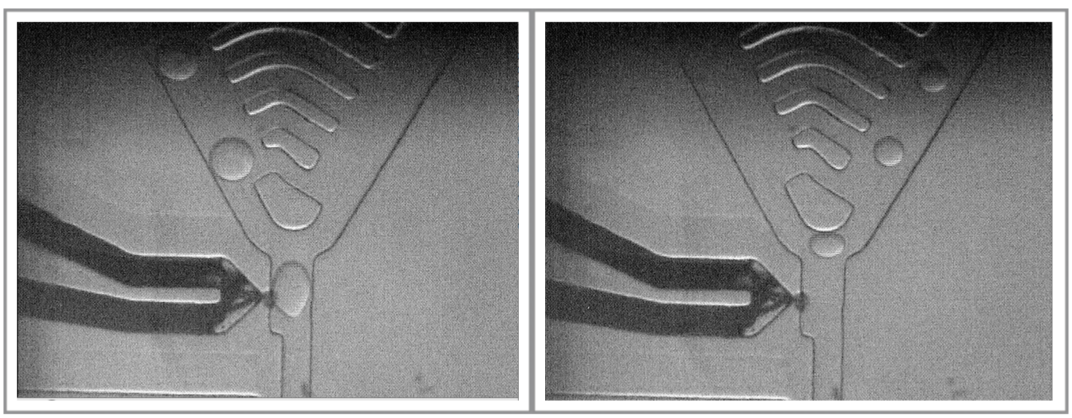

Fig. 15. Demonstrated droplet redirection with 1000V/20kHz applied signal (left) and when signal was turned off (right) - 1000V-20kHz.avi

Droplet redirection was not able to be demonstrated with the flat electrode designs but it was demonstrated with the sharp electrode design (see data files in USB key included with report). Due to the frame rate of the camera (30 fps), we could not ascertain the rate of droplet actuation. Slowing down the video, the droplet flow rate is estimated to be on the order of at least 100Hz. Not all droplets were observed to flow uniformly into one channel, There was no noticeable difference in performance of droplet redirection when the applied signal operated at 500Hz, 1kHz or 20kHz. Here 20kHz is assumed to be similar to a DC voltage, since the output signal has been significantly clipped high. To determine the effect of a higher frequency AC signal (20kHz), a more suitable switch is required.

With polydispersity in the re-injected droplets, when 500V was applied the chip was able to sort smaller droplets (30um diameter) while not drawing in larger droplets (45um diameter). This suggests an application where a continuously applied voltage could act as a filter to sort droplets based on size.

Videos of all cases tested can be found on the USB stick included with this report.

2.0 Conclusions

This project sought to add droplet redirection to a microfluidic sorter chip developed by a previous APSC 459 group. An technique for fabricating electrodes was determined, adding additional microfluidic channels upstream of a junction leading to the collection channels and filling them with low-melting-point alloy. Electrode designs were modeled in COMSOL and the previous group's sorter chip redesigned accordingly to include the most effective designs.

A high-voltage switch was obtained from the PHAS E-LAB, though it can only switch high voltages at a maximum of 1kHz, much less than the desired frequency of 20kHz. A few methods of increasing this switching frequency were suggested by the PHAS E-LAB and included in the recommendations.

Droplet actuation was demonstrated on the order of 100Hz with an applied voltage signal between 500V - 2500V AC with a frequency range of 0-1kHz.

In order to attain fluorescence-based droplet sorting at appreciable speeds (1-2kHz), more work is required in the following areas:

1. Actuation needs to be coupled to the first APSC 459 group's droplet detection system. The LabVIEW scripts would need to be modified and extended to drive the HV switch.
2. A new HV switch which could operate in the 20kHz range would need to be sourced or the current switching setup improved. The effect of a high-frequency high-voltage signal would then need to be tested.
3. Droplet generator-sorter coupling would need to be improved to increase control over droplet speed in the sorter chip.

3.0 Project Deliverables

3.1 List of Deliverables

Deliverable	Medium	Details
COMSOL Models	Electronic	Finite-element analysis of different electrode designs
Droplet Actuation	Electronic	Videos of droplet actuation (video)
Microfluidic design	Electronic	AutoCAD file with modified chip design
Microfluidic chips	Physical	Microfluidics chips with electrode channels
Photolithographic masks	Physical	Mask fabricated during project
Photoresist molds	Physical	Molds fabricated during project
HV switch	Physical	Was borrowed from Pavel, but he can help construct copies
Log Books	Paper	Records of meetings, rough work
Recommendation Report	Paper/Electronic	Submitted after project is finished.
Presentation	In Person	Given after project is finished.

3.2 Financial Summary

#	Description	Quantity	Vendor	Cost ($ CAD)	Purchased by	To be funded by
1	Eutectic Gallium Indium SKU-pack size: 495425-5G	1	Sigma-Aldrich	80.30	Hansen Lab	Hansen Lab
			Total	80.30		

4.0 **Recommendations**

4.1 Electrode Fabrication

Currently electrodes are fabricated by injecting eutectic Gallium-Indium (melting point 15.7 ^oC) into the electrode channels. This is done easily with a 1mL syringe, but there are several drawbacks:

1. GaIn is toxic and can cause severe skin burns, making fabricated electrodes more difficult to handle. It is also difficult to clean off surfaces.
2. GaIn is difficult to inject – flowing the GaIn through 30um-wide channels requires a large enough back pressure such that removal of the syringe from the channel inlet will release a large amount of GaIn from the syringe. Not only a waste of material, even when cleaned off the PDMS remains slightly opaque, reducing image quality with the optical system.
3. The HV and ground voltages are connected to the electrode channel by directly inserting a header pin into an electrode channel, which causes the GaIn near the oil channel to shift and pull away if the pins are inserted/removed. This affects the uniformity of the electric field generated.
4. GaIn will expand and contract readily with changes in temperature. Bringing the chip into an environment warmer than that in which it was made will cause the GaIn to spill out of the electrode channel outlets as well as pull away from the walls. If the header pins have been attached to the chip via an adhesive, this expansion will cause the adhesive to lift from the chip.

Use of a low-melting point alloy whose melting point is above room temperature (60-70^oC) could easily address all these concerns. Of the alloys investigated, Wood's alloy seems to be the most feasible in terms of cost ($92.22 from City Chemical LLC as opposed to $355 for Indalloy 19 from Indium for the minimum order). This project would only require a minimal amount and the PHAS E-LAB has agreed to purchase any excess Wood's Alloy.

4.2 Droplet Re-injection

Droplet re-injection into the sorter chip is difficult and erratic using syringe pumps. Several concerns came up:

1. Droplets must be withdrawn from an external container using a syringe. This causes some droplets to be left as residue in the container as well as risks having some droplets coalesce when drawn through the syringe tip.
2. Back pressure during re-injection is difficult to control, complicated by relatively long tubing between the syringe pump and the chip with changes in height. Often times it was necessary to apply a large back pressure then switch it off and have the residual pressure drive the droplets in order
3. Droplets, being less dense than the HFE-7500 oil environment are positively buoyant and will clump at the highest point in a loop of tubing. This requires a larger back pressure to drive droplets and results in the droplet injection speed being sometimes unpredictable.

The system in the Agresti paper has both droplet generator and sorter on the same chip; droplets are formed and flow through a stretch of polyetheretherketone tubing directly to the sorter. Having an integrated generator/sorter chip would address some of the issues surrounding re-injection.

4.3 HV switching

Currently, the maximum operating frequency of the switch provided by the PHAS E-LAB is approximately 1kHz at best, due to the large time constant of the signal output. In order to properly test dielectrophoresis with a HV AC signal (on the order of 20kHz or greater), an alternative switching method is required. Pavel Trochtchanovitch from the PHAS E-LAB has several alternatives which could be explored:

1. Using a second switch to sink current from the signal electrode as soon as the first switch is turned off. This would involve an additional interface circuit which prevents the two switches from being turned on at the same time, with some tunable "dead-time" between when the operation of the switches. Of course, this dead-time will be a limiting factor on the maximum operating frequency of the dual-switch setup.
2. Building a switching circuit from gate drivers instead of opto-isolaters. This design would be limited to ± 600V, so a bipolar HV source would be required.

5.0 Appendices

Appendix A: Fabrication Protocols

A.1 Wafer Fabrication Procedure

1. Clean the surface of the silicone wafer
    a. Pour IPA solution onto both sides of the silicone wafer
    b. Use nitrogen gas to dry the wafer
2. Pour photoresist onto the wafer
3. Set wafer on the spin-machine
    a. Turn on the vacuum and ensure the wafer is secured
    b. Set up the protocol
4. Start the spin-machine and wait
5. Bake the wafer in the oven
6. Ultraviolet exposure
    a. Attach the mask on a glass slide
    b. Place wafer in the frame
    c. Line up the wafer with the mask using the microscope
7. Expose the wafer in ultraviolet
8. Develop the wafer
    a. Pour the developer in a container
    b. Place the wafer in the liquid and rinse
    c. In a separate container, rinse the wafer again with the same developer
9. Bake the wafer in the oven
10. Examine the wafer under a microscope to make sure no unwanted dust particles are present
11. Measure the height of the oil channel

A.2 Wafer Fabrication Protocols

Name:	Adam Q / Luke
Date:	07-Feb-12
Photoresist:	SU-8 3050 Lot# 11040263 Expiriry 5/1/2012
Previous layers:	Should have done IPA coating before resist
Spin speed and time	500rpm spread cycle for 10s, 3250 rpm for 30 seconds
Pre-bake (time and temperature)	95 C 15 min
Exposure time:	9s w/ filter
Post-bake time:	1-5-1 65-95-65
Developer:	SU8 Developer
Development time:	2 min
Solvent to wash off developer:	IPA
Hardbrake:	Ramp to 120C, hold 10 mins, ramp down
Thickness (using alpha-step)	37-40 (µm)
Other notes:	Some of the electrodes are touched the oil channel. May be the result of under-developing

Name:	Adam Q / Luke / Sam
Date:	07-Feb-12
Photoresist:	SU-8 100 (lot 11080530, exp 9/1/2012)
Previous layers:	Su8 3050
Spin speed and time	500 rpm for 30s, 1600 rpm for 50s
Pre-bake (time and temperature)	65 for 20 min, 95 for 50 min, 65 for 5 min
Exposure time:	26 sec with filter
Post-bake time:	n/a
Developer:	SU8 developer
Development time:	8 min
Solvent to wash off developer:	Ipa
Hardbrake:	None
Thickness (using alpha-step)	n/a

Other notes:	Forgot to tape over alignment marks on previous layer so alignment was very difficult

Name:	Adam Q / Luke / Sam
Date:	09-Feb-12
Photoresist:	SU-8 100 (lot 11080530, exp 9/1/2012)
Previous layers:	SU8 3050, SU8 100 (removed)
Spin speed and time	500 rpm for 30s, 1600 rpm for 50s
Pre-bake (time and temperature)	65 for 20 min, 95 for 50 min, 65 for 5 min
Exposure time:	26 sec with filter
Post-bake time:	65 for 2 min, 95 for 12 min, 65 for 2 min
Developer:	SU8 developer
Development time:	8 min
Solvent to wash off developer:	IPA
Hardbrake:	None
Thickness (using alpha-step)	130μm
Other notes:	

A.3 PDMS Chip Fabrication

1. Use TCMS to remove moisture from silicone wafers under a fume hood
2. Make a foil dish for each wafer
3. Place each wafer in foil dish
4. Apply PDMS cleaning layer to remove any particles
    a. Mix PDMS using 10:1 ratio of RTV A:B with 20g A and 2g B per wafer
    b. Mix in centrifuge (1 minute mix plus 2 minute degas)
    c. Pour onto wafer
5. Bake at 80C for 25 minutes
6. Remove cleaning layer
    a. Cut along edge of water using a scalpel
    b. Peel off PDMS
7. Apply thicker PDMS layer
    a. Mix PDMS using 10:1 ratio of RTV A:B with 50g A and 5g B per wafer
    b. Mix in centrifuge (1 minute mix + 2 minute degas)
    c. Pour onto wafer
8. Place PDMS with wafers in a vacuum chamber for 1 hour
    a. Bubbles will form, so alternate at beginning between vacuum and atmospheric pressure to ensure PDMS will not bubble over sides of foil dish
    b. After bubbling subsides, wafers can be left in vacuum chamber for the remainder of the hour
9. Bake at 80C for 1 hour
10. Punch holes for channel inlets and outlets

Appendix B: SOP for generating droplets for use with 20-67-16 (D1-D2-Height) droplet generator chip.

1. Flush droplet generator with distilled water.
2. Check for presence of debris; if present, flush again with water.
3. Set up syringe pumps
    a. Withdraw distilled water and HFE-7500 oil with 3% w/w Raindance surfactant into 1mL syringe.
    b. Attach tubing long enough to reach generator chip to end of syringes; inject liquid to tips of tubing.
    c. Connect tubing to appropriate inlets.
    d. Set syringe diameter (4.83mm if using 1mL syringe).
    e. Set flow rate to 25uL/hr for water, 250uL/hr for oil.
4. Turn on pump for water, ensuring that
5. After 5 min, turn on pump for oil.
6. With generator outlet open, use optical setup and LabVIEW program to ensure that correctly sized droplets are being outputted.
7. Attach a short piece of tubing to generator outlet and redirect droplets into a microcentrifuge tube (or container of choice) for storage.

Appendix C: HV Switch design by the UBC PHAS E-LAB

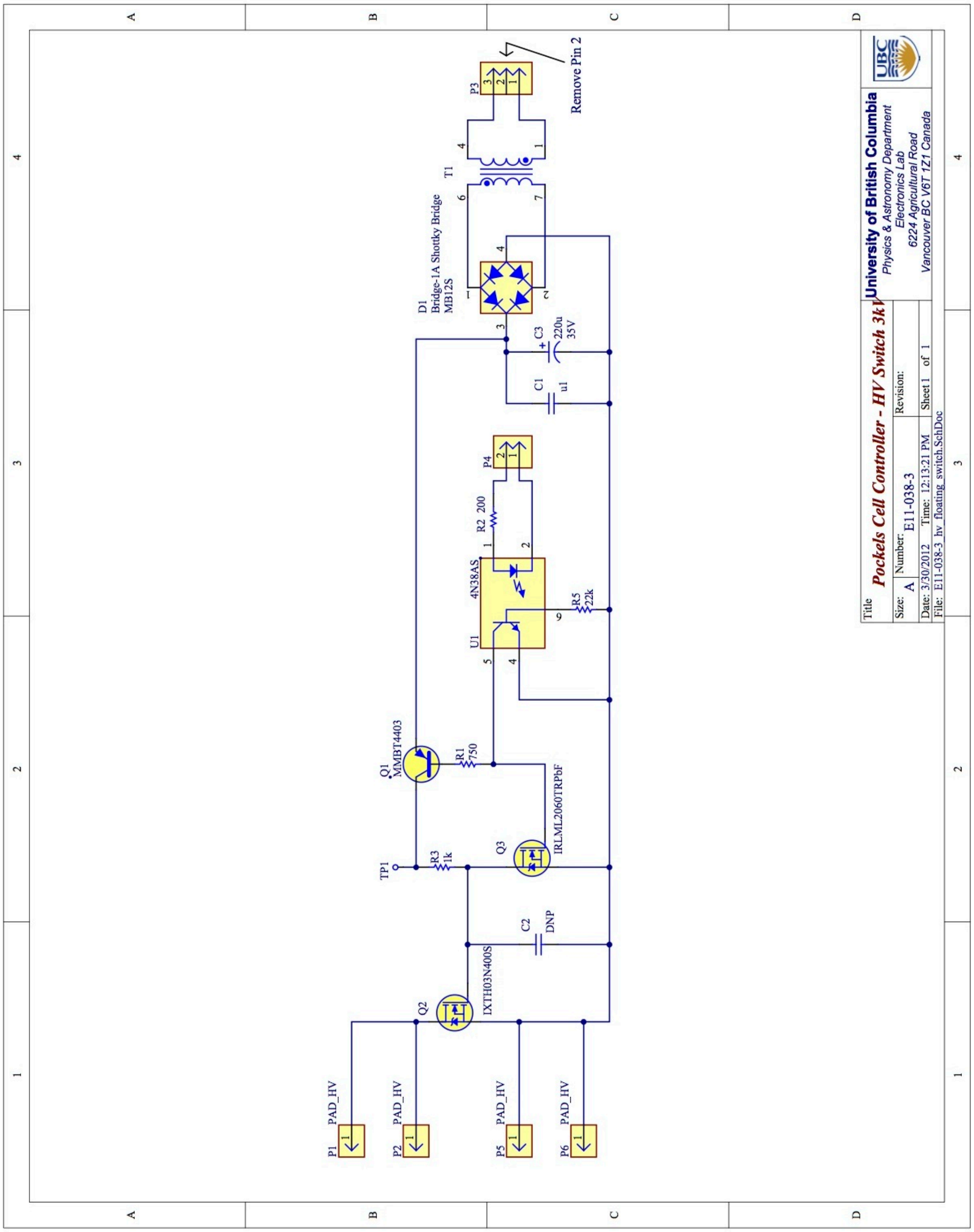

The switch transistors Q1 and Q2 are driven by an applied TTL signal (0-5V), optically isolated with U1. The signal is propagated through to the 3N400S high-voltage MOSFET whose drain-to-source voltage is rated as being up to 4kV. The MOSFET begins to conduct when the gate-to-source voltage exceeds 2~4V, resulting in the voltage at P5/P6 being the same as that at P1/P2. C2 has been removed to allow for faster switching.

Appendix D: Electrode alloy quotes

AIM Solder

Gmail - Low melting-point solder quote. 12-04-02 7:37 AM

Samuel Wu <samuelwu90@gmail.com>

Low melting-point solder quote.

Gaby Melki <gmelki@aimsolder.com> Wed, Feb 29, 2012 at 11:28 AM
To: Samuel Wu <samuelwu90@gmail.com>
Cc: Claude Carreau <ccarreau@aimsolder.com>

Hello,

Following is the quote for the solder wire you requested:

Alloy: 49Bi/21In/18Pb/12Sn
Diam.: 0.030"
Min qty: 10 feet
Price: $45.90/ft
Lead time : 10 working days or sooner
FOB : Montreal
Terms: COD

Regards,

Gaby Melki
Customer Service Manager
AIM Metals & Alloys L.P.
Tel : 514- 494-5502 * 800-361-0783
Fax: 514- 494-6133 * 800-363-7754
gmelki@aimsolder.com
www.aimsolder.com
"Solder Plus Support"

From: Samuel Wu [mailto:samuelwu90@gmail.com]
Sent: Wednesday, February 29, 2012 12:56 PM
To: Gaby Melki
Subject: Low melting-point solder quote.

[Quoted text hidden]

https://mail.google.com/mail/u/0/?ui=2&ik=288eee50d0&view=pt&q=solder&qs=true&search=query&msg=135ca9579228772c Page 1 of 1

THE INDIUM CORPORATION OF AMERICA®

QUOTATION

Customer:	9027944 Samuel W. University of British Columbia Dept. of Physics AMPEL, Room 245 2355 East Mall Vancouver BRC V6T 1Z4 Canada Phone: 604-961-1530	**Page:**	1
		ICA Contact:	ble
		Customer RFQ #:	
		Quote Date:	02/23/12
		Expiration Date:	03/02/12
		Terms:	Prepay (c/card
		Delivery Terms:	Free car Utica, NY
		Customer Currency:	US$ US Dollar
		ICA Territory:	BritColm
		ICA Estimate:	E016093

* Effective 01 Jan 2011: Shipping terms based on Incoterms 2010®, unless otherwise stated. *

Item / Description	Quantity	UM	Unit Price	Net Amount
Ind#19 Solder Wire	28.000		12.71000	355.88
.030" dia. wire		GM		
Min. order 28gm @ $12.71/gm				
lead time: estimated 12-15 working days after ARO				
single release				

Sale Amount:	355.88
USA Tax:	0.00
GST/VAT:	0.00
Misc:	0.00
Total Amount:	355.88

Please contact us immediately to discuss
any issues with this correspondence.
Thank you for your business.

INDIUM

THE INDIUM CORPORATION OF AMERICA®

www.indium.com
askus@indium.com
PRC +86 (0)512 628 34900
SINGAPORE +65 6 268 8678
UK +44 (0) 1908 580400
USA +1 315 853 4900

ISO 9001 REGISTERED

Y002-007.RVF 10 FEB 2011

6.0 References

Agresti, J. J., Antipov, E., Abate, A. R., Ahn, K., Rowat, A. C., Baret, J.-C., Marquez, M., et al. (2010). Ultrahigh-throughput screening in drop-based microfluidics for directed evolution. *Proceedings of the National Academy of Sciences of the United States of America*, *107*(9), 4004-9. National Acad Sciences. doi:10.1073/pnas.0910781107

Ahn, K., Kerbage, C., Hunt, T. P., Westervelt, R. M., Link, D. R., & Weitz, D. A. (2006). Dielectrophoretic manipulation of drops for high-speed microfluidic sorting devices. *Applied Physics Letters*, *88*(2), 024104. doi:10.1063/1.2164911

Behlke. Fast High Voltage Transistor Switch: 61-31-GSM - Datasheet. Retrieved April 1, 2012 from Behlke website: http://www.behlke.de/pdf/61-03-gsm.pdf

Griffiths, A. D., & Tawfik, D. S. (2006). Miniaturising the laboratory in emulsion droplets. *Trends in biotechnology*, *24*(9), 395-402. doi:10.1016/j.tibtech.2006.06.009

Mulholland, B., da Costa, D., & Eldridge, D. (2010). *Ultrafast Microfluidic Drop Sorter*. *Alternatives*.